Dynamics in Carbon Nanotubes for In-Materio Computation

Stefano Nichele, Johannes Høydahl Jensen, Dragana Laketić, Odd Rune Lykkebø and Gunnar Tufte

Department of Computer and Information Science
Norwegian University of Science and Technology
Trondheim, Norway
Email: {nichele, johannj, draganal, lykkebo, gunnart}@idi.ntnu.no

***Abstract*—In-materio computation exploits physical properties of materials as substrates for computation. Evolution-In-Materio (EIM) uses evolutionary search algorithms to find such configurations of the material for which material physics yields desired computation. New unconventional materials have been recently investigated as potential computational mediums. Such materials may intrinsically possess rich physical properties, which may allow a wide variety of dynamics. However, how to access such properties and exploit them to carry out a wanted computation is still an open question. This article explores the dynamics in one particular type of nanomaterials which is used to solve computational tasks. Nanocomposites of Single-Walled Carbon Nanotubes (SWCNTs) and PolyButyl MethAcrylate (PBMA) are configured so as to undergo evolutionary processes with the goal of performing certain computational tasks. Early experiments showed that rich dynamics may be achieved, which may yield complex computations. Some indications of chaotic behavior were observed so further work was carried out with the aim of examining the dynamics achievable by such nanocomposites. Since it is not an easy task to access the physics at the very bottom of the material, investigation of the material dynamics is kept within the limits imposed by our measurement equipment and the level of observability enabled by it. Presented results show that interesting, complex dynamics is achievable by examined nanocomposites and that it depends on the type of signals used for the material configuration as well as on the material intrinsic properties such as percentage of SWCNTs in the nanocomposite.**

***Keywords*–Computation-in-Materio; Evolution-in-Materio; Evolvable Hardware; Carbon Nanotubes; Dynamical Systems; Complexity.**

I. Introduction

Computations result from perturbations of some dynamical system. The observable output of the system is the result of its dynamics. Dependent on the type of dynamics exhibited by the system, computations of various complexity levels may be achieved. The type of dynamics depends on the physics of the system and on the way in which the system is manipulated. Our work considers novel nanoscale materials [1] and was carried out within the EU-funded NASCENCE (NAnoSCale Engineering for Novel Computation using Evolution) project [2]. The nanomaterials investigated within the project are nanocomposites of Single-Walled Carbon Nanotubes (SWCNTs) and polymer molecules (PBMA), and networks of gold nanoparticles. The investigation of nanocomposites is performed under the Evolution-In-Materio (EIM) scenario [3], [4].

EIM is a novel approach to designing computing devices where various materials are used as computational substrates. It is one approach that may emerge as an answer to the challenges of today's widely accepted semiconductor technology. Digital computers based on silicon technology are designed using a conventional top-down process by human engineers. Engineering of such processors poses technological challenges due to scaling down. Various design techniques are applied in order to sustain scaling down of the semiconductor technology but it is becoming increasingly difficult to fabricate transistors at the nanoscale.

This has motivated efforts towards novel technologies that will assume not only new computational substrates but also novel principles of the design of computing devices and their usage. EIM is a bottom-up approach in which the physics of a computing substrate is used to produce computations of interest. Different computational substrates have been previously explored such as liquid crystals and Field Programmable Gate Arrays (FPGAs) [5]–[7]. The configuration of the computing substrate, i.e., some material, undergoes evolutionary changes until some desired response of the material is achieved according to the computational task at hand. The digital computer accesses the material via a special board, which allows the Evolutionary Algorithm (EA) to apply configuration and input signals and read the material response which will guide the evolutionary search.

Figure 1 illustrates an EIM system. Three main entities can be distinguished: a digital computer, the material and the interface between the two. The system clearly shows the separation of an analog/physical domain in which materials operate and a digital domain in which the computer responsible for input/output mapping and configuration operates. In all such systems an interface is needed for bidirectional translation of signals between digital signals of the computer and analog signals in the physical domain of the material. As mentioned, the digital computer is used for running the EA, which generates a population of genomes, and translates each genome into suitable analog signals which can be sent to the interface board.

Further, the response of the material for a given configuration and input signals is translated from analog form as produced by the material to its corresponding digital value so that the computer can calculate the fitness value of the genome. The fitness value guides evolutionary search towards a solution to the problem at hand.

In order to produce interesting behavior under the EIM scenario, it is required that the material is able to exhibit rich dynamics. The richness of the exhibited dynamics can be attributed to the physical properties of the material. In a

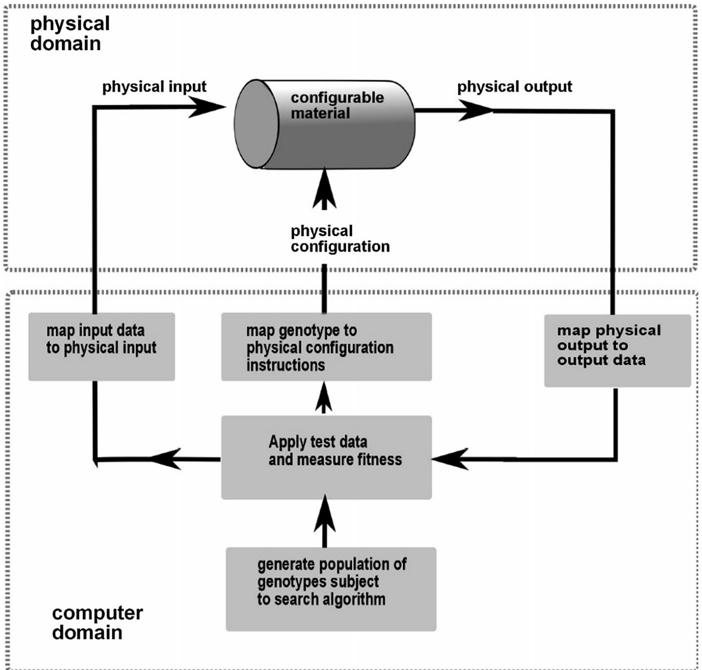

Figure 1. Principle of EIM illustrating the separation of an analog/physical domain where the material operates and the digital domain of computers, from [3].

way it can be said that EIM manipulates the material so as to produce rich dynamics. The material blob is treated as a black box and EAs are used to "program" the material to solve a problem at hand.

Such a black box hybrid approach has been shown successful for a number of computational problems [8]–[13]. At the current state of research, it is not clearly understood what the exploited physical properties are and what the best way of exploring them is, e.g., what number of inputs and outputs and which types of signals - electrical (static voltages, sinusoidal waves, square waves) or even of some other kind such as temperature or light. The solved problems serve as a proof of concept that an EIM approach may be used for solving computational problems and indicates that it may be competitive in terms of computational time, size, and energy consumption. However, scaling-up to solve larger instances of a problem requires a better understanding of the dynamics exhibited by the material. In other words, the black box needs to be opened so that the underlying physical properties of the material are well understood. The number of used input electrodes, configuration signals available, etc. will directly affect the evolutionary search space.

Observing dynamics and its emergent complexity in computational materials is not an easy pursuit. Observability is limited by what output can be measured from the material and at which scale. At some scales we are not able to directly observe physical effects present in the materials, e.g., quantum effects due to mechanisms of electron transmission through carbon nanotubes. Therefore, we are limited to use signals which can be observed and measured. Figure 2 illustrates the taken approach to observe, exploit and gain an understanding of the dynamics of EIM systems. At the lowest level we have the physics of the material where computations happen, but

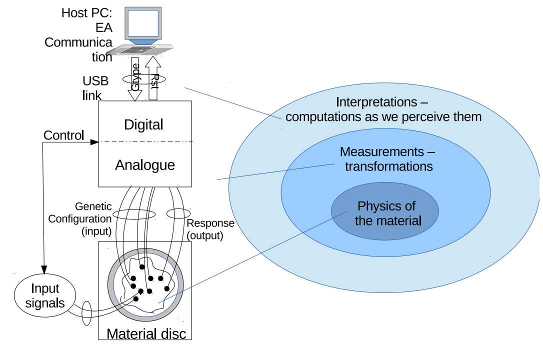

Figure 2. Conceptual domains of the computing system.

due to nanoscale and even quantum effects, what is captured by our instruments will at best be just an approximation. In other words, the lowest level is inaccessible and must be treated as a black box. At the second level, the level of measurements and transformations, physical properties and dynamics are observable in the analog domain. This level can be explored to gain insight into the electrical properties of the material. The top level is the level of interpretations, i.e., computations as we perceive them. So, as shown in Figure 2, the dynamics of the analog signals are interpreted and transferred to data, i.e., the computational input – output mapping is performed. The top level is the level which is explored for computation. Here, it is important to note that the observations on the top level emerge as a result of all underlying dynamics.

The work presented in this paper includes a specific approach, as illustrated in Figure 2, to investigate the dynamics of the material at hand. The approach considers the complexity of the input - output mapping performed by the material for computation. Complexity is hard to measure even when well defined as, for example, Kolmogorov complexity [14]. Some approximations are needed if we want to obtain quantitative measures. In this work, we adopt *compressibility* as a measure of complexity.

This paper, which is an extended version of [1], is organized as follows: Section II provides background on EIM and position of the NASCENCE project within the field. Section III presents experimental platform Mecobo, which was developed within NASCENCE project, and which is used in our EIM experiments. Also, an experimental setup is explained as well as the material which was used in the experiments. Moreover, the section provides some background on different computational domains which can be distinguished under EIM computing scenario. Further, Section IV provides some initial results, presented in [1], which demonstrate interesting behaviors of the investigated material. Section V presents experiments which were conducted with the aim of investigating material dynamics in a greater detail. A measure of complexity is introduced which is used as the description of material behavior, the three sets of experiments are described followed by the results and the discussion which relates results to theoretical foundations. Finally, Section VI provides conclusion about the presented experiments and exhibited material dynamics within EIM computing.

II. Background – Evolution-in-Materio

The term Evolution-in-Materio was introduced by Julian Miller and Keith Downing in 2002 [4]. The general concept of EIM is that physical systems may intrinsically possess properties which may be exploited for computation.

A. Pioneering work

Early work on manipulation of physical systems for computation is related to the work of Gordon Pask [15], a classical cyberneticist whose pioneering work dates back to the 1950s. He tried to grow neural structures, dendritic wires, in a metal-salt solution by electrical stimulation [7]. His goal was to self-assemble a wiring structure within the material in order to carry out some sort of signal processing embedded in the material. He was able to alter the position and structure of the wiring filaments, and thus the behavior of the system. This was achieved by external influence, which consisted in applying different currents on electrodes in the metal-salt solution. This early version of material manipulation was done without aid of computers and different electrical configurations were tested manually. Stewart [16] later defined such a process as manufacturing logic "by the pound, using techniques more like those of a bakery than of an electronics factory".

B. Analog computers, FPGAs and liquid crystal

Later, Mills constructed an analog computer which he called Kirchhoff-Lukasiewicz Machine (KLM) [17]. The construction was done by connecting a conductive polymer material to logical units. The analog computation was carried out by placing current sources and current sinks into the conductive foam layer and reading the output from the logical units. One could argue that such machines were not easy to program due to the manual placement of connections into the material. On the other hand, some advantages of performing computation directly in the material substrate became obvious, e.g., a large number of partial differential equations were solved within nanoseconds.

In 1996, Thompson used intrinsic evolution to produce electrical circuits in FPGAs [5]. In his well-known experiment, he demonstrated that artificial evolution can be used to exploit physical properties of FPGAs to build working circuits, e.g., a frequency discriminator circuit. He found out that placing the circuit in a different part of the chip or disconnecting some unused modules would result in a non-working solution. Moreover, he was unable to replicate the chip behavior in simulation because evolution had exploited underlying physical properties of the FPGA. In fact, changing the FPGA with a similar model from the same producer would result in slightly different behavior. Thompson described such a process as "removing the digital design and letting evolution do it".

In [4], Miller and Downing suggested several materials which may be suitable for EIM, liquid crystals being among them. Simon Harding [18] later demonstrated that it was indeed possible to apply EIM on liquid crystals to evolve several computational devices: a tone discriminator [19], logic gates [20], and robot controllers [6]. Liquid crystal is a movable material where voltages affect orientation of the crystals. The movability was problematic since the material would undergo permanent changes during evolution. This led to unstable solutions that worked only once. Nevertheless, he showed that it was possible to quickly reach a working solution again by re-running the evolutionary algorithm for a couple of generations [19].

C. The NASCENCE project and recent work

Recently, the NASCENCE project [2] addressed nanomaterials and nanoparticles for EIM with the long term goal to build information processing devices exploiting such materials without the need to reproduce individual components. In particular, investigated nanomaterials included nanocomposites made of SWCNTs and polymer molecules and nanoparticle networks, in particular gold coated nanoparticles. Several hard-to-solve computational problems have been solved as proof of concept, e.g., Traveling Salesman [8], logic gates [9], bin packing [10], machine learning classification [11], frequency classification [12], function optimization [13] and robot controllers [21]. The SWCNT materials from the project are the subject of our investigation in this paper.

D. Interpretation and computation

As stated, EIM has been used to solve a variety of problems. However, these results are all limited to a specific problem domain. To assess the potential computational power available in a material, we need a more general measurement. One way is to view *complexity* as indication of potential computational power [22].

Kolmogorov complexity [14], [23] is well-defined but incomputable in theory. However, it is possible to use measures such as compressibility to approximate complexity to some extent [24]–[27]. In fact, strings that are hardly compressible have a presumably high Kolmogorov complexity. Complexity is then proportional to the compression ratio.

High measurable complexity of output data or a high complexity ratio between input and output data may not always be a desired property. In classifier systems, such as Thompson's frequency discriminator [5], the output may be a binary response to a complex input signal. In this case the complexity ratio between output and input is very low. However, the computation, i.e., internal state transitions in the underlying physics of the material, is still a complex process but the complexity is unobservable since we only observe the input and output signals.

III. A platform for experiments and understanding of EIM systems

The conceptual idea of exploiting physics for computation requires a physical device, i.e., the material. In most EIM works, an intrinsic approach has been taken – computation is a result of real physical processes and the evaluation is a result of the performance of a physical system. An intrinsic approach allows access to all inherent physical properties of the material [3]. An analog computation [28] is a possibility, however, in this work a hybrid approach is taken. The hybrid approach includes the computational matter in a mixed signal system using a digital computer to configure and communicate with the material. Such an approach enables the computational power of the material with the ease of programmability of digital computers [2]. In a hybrid approach, observability is an issue, i.e., ensuring that the data from the material is observable and sound without using more computational power for the observation than the actual computation [29].

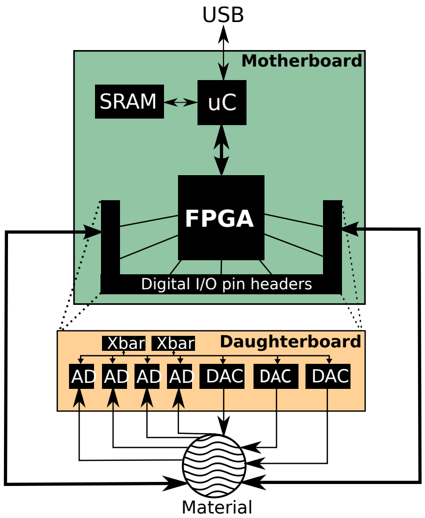

(a) Block diagram of the Mecobo hardware interface.

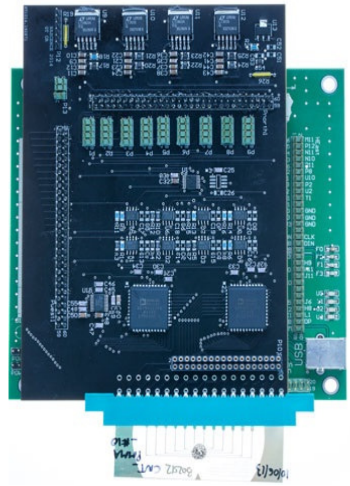

(b) Picture of the Mecobo motherboard with mixed signal daughter board.

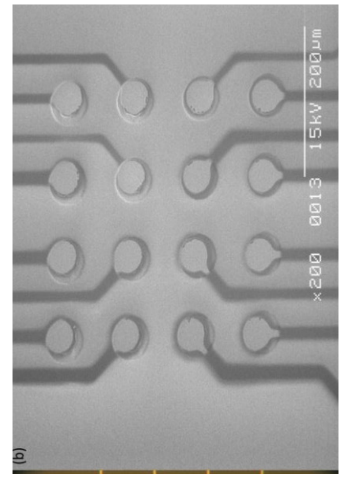

(c) Electrode array, microscopic view. (Source: documentation of the NASCENCE project).

Figure 3. Overview of the Mecobo hardware interface.

A. NASCENCE's Mecobo: an experimental platform for EIM

A hybrid approach requires an interface between the digital world of computers and the analog world of materials. The Mecobo experimental platform [30] from the NASCENCE project is a hardware/software platform implementing the conceptual Evo-Materio-system shown in Figure 1.

Figure 3 shows an overview of the hardware interface: a Mecobo platform and microelectrode array on the material slide. A block diagram of the Mecobo platform is shown in Figure 3a. Configuration specification, i.e., genotypes, are loaded from a PC to Mecobo over a USB port. A micro-controller communicates with the USB interface and with an FPGA via an internal bus. The FPGA can be interfaced to the materials directly or, as shown in the figure, use a daughter board to extend the range of possible signals.

A picture of the Mecobo hardware is presented in Figure 3b. In the picture, the Mecobo is shown with a mixed signal daughter board and a material sample on a glass slide plugged in. Electrical connection between the material on the slide and the board is realized by the microelectrode array. A microscopic view of the microelectrode array before material disposition is shown in Figure 3c.

Mecobo is capable of controlling close to 100 individually configurable input/output signals (pins), which can be connected to the material. Each signal is described by parameters at a given point in time. For example, a pin can be programmed as a recording pin from time 0 to $100ms$, or as an output pin of square waves of some frequency from 0 to $1000ms$, or as an output pin of a constant voltage level, e.g., $2.7V$ from time 0 to $1500ms$ etc. Mecobo is connected to a host PC over USB and communicates via a Thrift server [31]. Communication based on Thrift technology also enables access to Mecobo remotely over the Internet. The maximum analog sampling frequency of the Mecobo board is $500kHz$. Input signals may be static voltages or periodic (e.g., square, sinusoidal) waves ranging in frequency between $400Hz$ and $25MHz$. For more details on Mecobo and an overview of the full range of programmable properties of the platform, see [30].

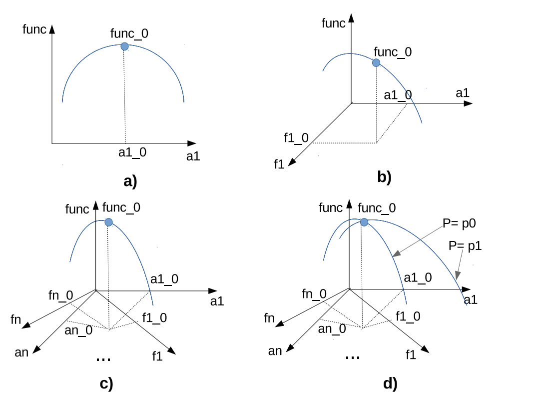

Figure 4. CNT computing system within a system theory framework.

B. Explaining computations within EIM

It can be said that computations are based on transformations of a system, so that the system input(s) and output(s) are related in some functional way. This functional relation can be expressed by a simple formula:

$$y = F(x) \tag{1}$$

where x and y correspond to an input and output of the system, respectively, and, in general, they are considered to be multidimensional and represented by vectors.

One way of analysis, more formally addressed within the system theory [32], [33] assumes that the system state is described by a set of variables that move through a state space.

For an EIM scenario, a better look into the state space of the system needs clarification of what is meant by system variables [34]. According to the explanation of different domains of computation as described in Section I, the variables of the system belong to the *domain of measurements* as schematically shown in Figure 2. The voltages and the set of properties which define them in this domain, i.e., amplitude, frequency and phase, can be represented with:

$$v_i = a_i \cdot func_p(f_i, \phi_i) \quad (2)$$

where v_i is voltage on the i-th electrode, a_i the amplitude, $func_p$ some periodic function, f_i frequency of the function $func_p$ and, finally, ϕ_i the phase of the voltage, all referring to the i-th electrode. The symbols are left lower case to remind that all of these values can be time varying.

Let us now consider an example in which for a system to perform functionality $func\_0$, for the input x_0, an output value y_0 is desired (Figure 4 a)). For simplicity, the variables on each of the axes are assumed to be scalars. When different configuration voltages are applied to the material, they change the system variables so that it passes through various states in the state space along some trajectory. Further, let us assume that only one electrode is used for configuration voltage and only one voltage parameter is changed, for example amplitude. By changing the amplitude along the a_1 axis different input-output mappings will be performed by the system. EIM would then search through the space until $func\_0$ point is reached. If also the frequency of the voltage v_1 is changed, then the state space could be searched along two axes as shown in Figure 4 b). And even further, if more than one electrode is used for configuring the material, then, in general, the space would look something like in Figure 4 c) and would be searchable along high number of axes, the limitation being only the physical number of electrodes in the system. Moreover, the state space may grow due to the change in some parameter, like temperature or light, as shown in Figure 4 d), which may all increase the size of the state space to search for the solution.

IV. A Detailed View of Material Dynamics

Experiments are performed on SWCNT mixed with PBMA on a micro electrode array supplied by Durham University. Material samples and micro electrode arrays are produced in a process where SWCNT-PBMA mixture is dissolved in anisole (methoxy benzene). The material samples are prepared on $4x4$ grids of gold micro-electrode arrays with pads of $50\mu m$ and pitch of $100\mu m$, see Figure 3c. The preparation is done by dispensing $20\mu L$ of the material onto the electrode area. The concentration of SWCNTs varies as shown in Table I where the material samples used in our experiments are listed. The SWCNT mixed with PBMA material dispersed over electrode array is baked for $30min$ at $90C^{\circ}$. The solvent dries out and leaves a thick film of immovable SWCNTs supported by polymer molecules. The substrate is cooled slowly over a period of 1h. This process leaves a variable distribution of nanotubes across the electrodes. Typically, carbon nanotubes are 30% metallic and 70% semi-conducting, while PBMA creates insulation areas within nanotube networks. Such electrical properties of the material may allow non-linear current versus voltage characteristics.

The coverage of gold microelectrodes with randomly dispersed nanotubes varies and some of the electrodes may even be left with little or no coverage, as visible in the Scanning Electron Microscope (SEM) image in Figure 5.

TABLE I. Different materials used in the experiments.

Material	SWCNT Concentration, $wt\%$
B09S12	0.53%
B15S03	1.25%
B15S04	1.50%
B15S08	5.00%

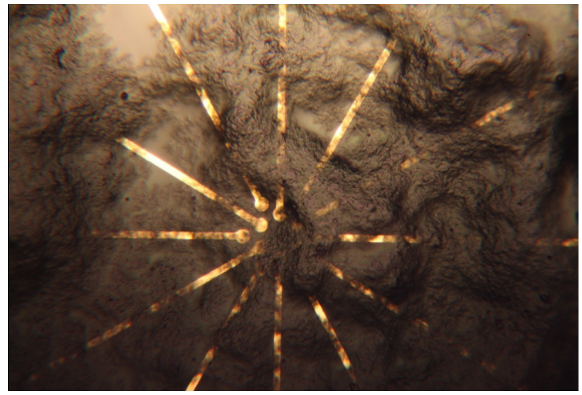

Figure 5. SEM image of gold electrode array with different coverage of nanotubes. Adopted from [9].

Initial investigation of the material response to various input signals showed several interesting behaviors in the material [1]. The goal was to gain insight into the material dynamics to identify suitable ways in which the material can be manipulated to perform computation.

As mentioned, EIM requires an interface between a digital computer which runs the EA and the material whose physics undergoes analog processes. This interface is typically provided by the Mecobo board. However, in order to better understand the underlying properties of the material and its responses, it is necessary to use more precise instruments. In these experiments, oscilloscopes and signal generators were used to get a more detailed view of the material dynamics.

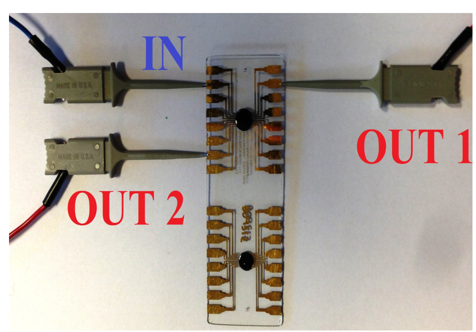

Figure 6. Material slide and pins connected to signal generator (IN) and oscilloscope (OUT).

A. Experimental Setup

In the experiments herein, we connect a material slide to a Hewlett Packard 33120A $15MHz$ function / arbitrary waveform generator (used as input) and an Agilent 54622D $100MHz$ mixed signal oscilloscope (used as output). Input signals are square waves at different frequencies from the signal generator and the output signals are recorded on the oscilloscope.

The input / output pins were chosen so that there would be an equal distance between microelectrode pads within the microelectrode array (Figure 3c). The placement of input and output signals on the material slide is shown in Figure 6, where the input probe (from the signal generator) is placed on pin #2 (IN) and the two output probes (to the oscilloscope) are connected to pins #9 (OUT1) and #7 (OUT 2).

B. Results and discussion

Figure 7 presents the experimental results. In particular, Figures 7a) show several snapshots of the material response on two different pins at different frequencies, ranging from $1KHz$ (Figure a1) to $14MHz$ (Figure a12). At $1KHz$ the signals may seem similar (a1), where the material charges-up and subsequently discharges, but in a zoomed in snapshot, i.e., where a part of the response is shown at a higher resolution (a2), a voltage spike is visible on the second probe which is not present on the first probe. This is better visible at $5KHz$ (a3), $30KHz$ (a4) and $100KHz$ (a5), where it is possible to notice that on the rising front there is a sudden voltage increase/drop. The material behavior is capacitor-like. Starting from $500KHz$ (a6), which is also zoomed in (a7), the second probe signal is similar to a square wave (most of the harmonic frequencies are passed) while the first probe acts more like a filter. The difference is caused by different concentrations of CNTs between the IN-OUT electrodes, i.e., different paths the current is enabled to follow between the electrodes. In both cases, there is a resonance phase which results in a deterministic yet semi-chaotic waveform. This may be the effect of some conducting sub-networks in the material that are enabled at specific frequencies and disabled at others. At 2, 5 and $8.5MHz$ the measured voltage decreases while frequency increases. At $10MHz$ (a11) a strange phenomenon is observed where both signals show a voltage increase. The effect is more prominent on the first output. We ascribe such behavior to be due to a feedback effect where harmonics of some frequencies are fed again into the material by some nanotube sub-networks. At $14MHz$ (a12) the signal on the second probe is sinusoidal, i.e., only one harmonic is present. As such, it may be concluded that with a single square wave input it is possible to observe a rich variety of behaviors while the frequency spectrum is traversed.

As the system produces uniform, stable, and semi-chaotic behaviors, it is of particular interest to visualize input-output responses and output-output relations in order to better understand traversed trajectories and attractors. For this purpose, XY plots are shown in Figure 7b), where OUT1 is plotted against OUT2 and Figure 7c), where IN is plotted against OUT1. In Figure 7b1), some orbits are present at $30KHz$. Similar orbits are visible at $60KHz$ (b2) and $100KHz$ (b3), moving towards opposite corners to those where the impulse is. After each impulse, there is a semi-chaotic orbit that relaxes before the next impulse arrives, as the semi-chaotic behavior is annihilated by the lack of energy in the material, until the arrival of the next impulse. This suggests that chaotic behavior may be present, yet particularly difficult to observe.

XY plots between input and output are shown in Figure 7c). These figures represent the phase space of the system (input-output pin pair). Figure 7c1) is obtained at $350Khz$. Several oscillating orbits are present, which are zoomed-in at $2MHz$ (c2). The same effect is observed for frequencies up to $5MHz$ (c3) while for frequencies around $10MHz$ and higher we observe a hysteresis loop, which indicates that some saturation may have been reached in the material. Some sort of non-linearity seems present, which is always a good indicator that the system may achieve complex behavior.

To summarize this set of results, even if a single square wave input signal is used, the resulting output shows a variety of behaviors. Square waves [35] produce richer dynamics than what may be achieved by a single static voltage or by a sinusoidal wave. Such richness of the response is due to the rich spectrum of the square waves which contains a variety of harmonics. In particular, some of the nanotube sub-networks may be sensitive to certain frequencies. Therefore, square waves may be better suited to penetrate the material and exploit the nanocomposite's intrinsic properties.

V. A Complexity View of Material Dynamics

The initial experiments with the oscilloscope measurements gave valuable insight into the different dynamics available in the material. However, such detailed measurements only give a very narrow view of the possible behaviors of the system. In order to get a broad picture of the space of possible material dynamics, one has to sacrifice some amount of detail. By using the Mecobo hardware platform (Section III) we are able to explore material dynamics at a higher level.

Mecobo allows us to scan a much wider range of signal frequencies, explore a myriad of different material locations and easily analyze the results on a PC. For these experiments we use the digital signal generator on Mecobo to generate square waves as input signals. The output signal is sampled as analog voltage using the on-board AD converter (Figure 3).

Complexity of the input/output signal is used as metric to classify different types of material dynamics. We use compressibility as an estimate of complexity as described in Section II-D. Since we are primarily interested in the complexity contribution of the material (and not the complexity of the input signal itself), we adapt the *complexity ratio*:

$$C_r = \frac{C_o}{C_i}$$

where C_o is the complexity of the output signal and C_i is the complexity of the input signal.

We present three sets of experiments where the computational complexity of the material is explored:

1) Complexity as number of input signals are increased
2) Complexity as function of one input frequency
3) Complexity as function of two input frequencies

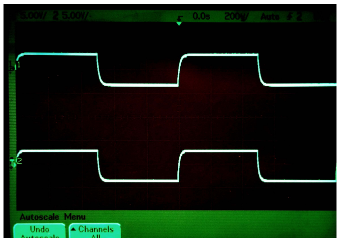
(a1) $1kHz$ (scale: $5V, 200\mu s$)


(a2) $1kHz$ (zoom, $2V, 5\mu s$)

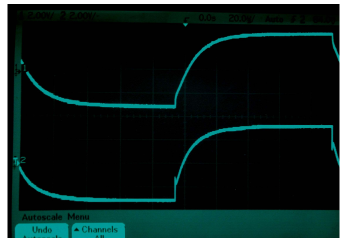
(a3) $5kHz$ (scale: $2V, 20\mu s$)

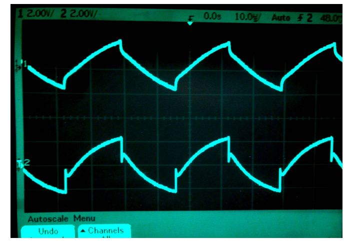
(a4) $30kHz$ (scale: $2V, 10\mu s$)

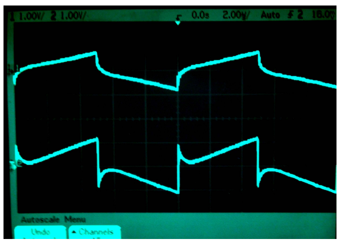
(a5) $100kHz$ (scale: $1V, 2\mu s$)

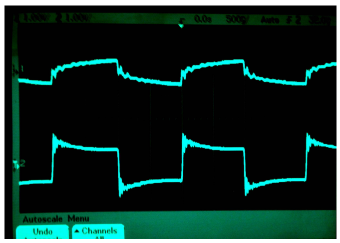
(a6) $500kHz$ (scale: $1V, 500ns$)

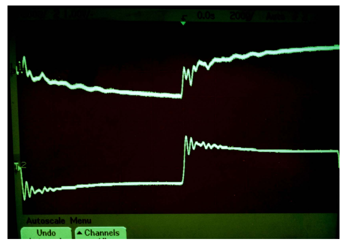
(a7) $500kHz$ (zoom, $500mV, 200ns$)


(a8) $2MHz$ (scale: $1V, 100ns$)

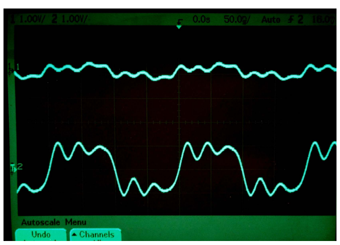
(a9) $5MHz$ (scale: $1V, 50ns$)

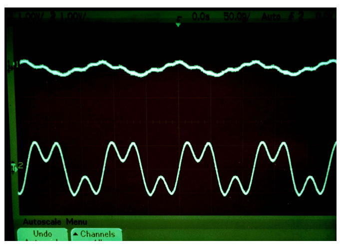
(a10) $8.5MHz$ (scale: $1V, 50ns$)

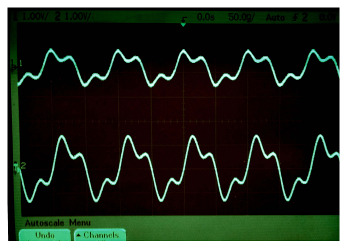
(a11) $10MHz$ (scale: $1V, 50ns$)

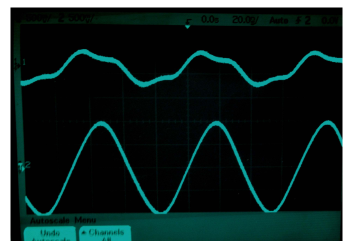
(a12) $14MHz$ (scale: $500mV, 20ns$)


(b1) $30kHz$ (scale: $1V, 1V$)

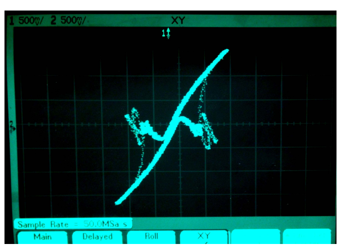
(b2) $60kHz$ (scale: $500mV, 500mV$)

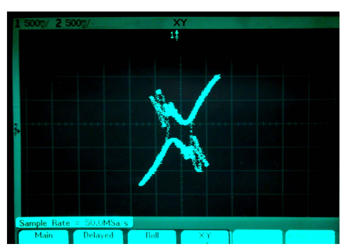
(b3) $100kHz$ (scale: $500mV, 500mV$)

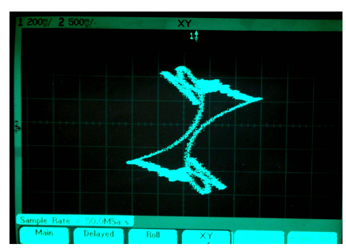
(b4) $500kHz$ (scale: $200mV, 200mV$)

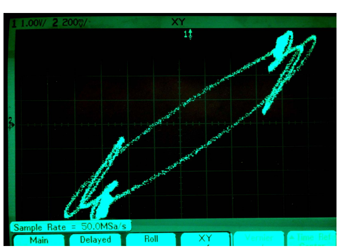
(c1) $350kHz$ (scale: $1V, 1V$)

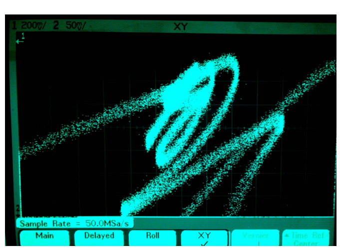
(c2) $2MHz$ (zoom, $200mV, 50mV$)

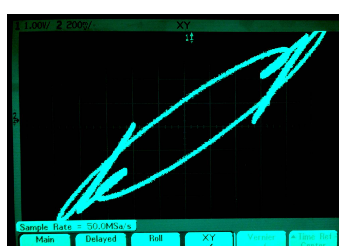
(c3) $5MHz$ (scale: $1V, 200mV$)

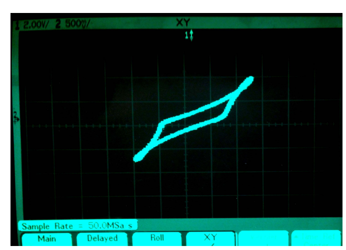
(c4) $10MHz$ (scale: $2V, 500mV$)

Figure 7. Oscilloscope screenshots. The resolution is indicated in parentheses. The resolutions have been chosen so as to be able to show interesting results at different scales.
(a) Voltage responses on 2 different pins with input square wave at different frequencies.
(b) XY plots, X (OUT1) is plotted against Y (OUT2) at different frequencies.
(c) XY plots, X (IN) is plotted against Y (OUT1) at different frequencies.

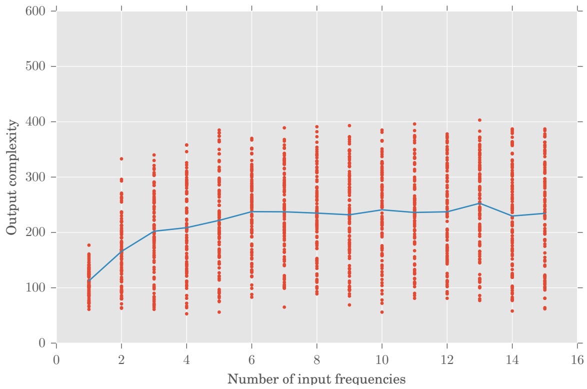

(a) Material B09S12 (0.53 wt% SWCNT)

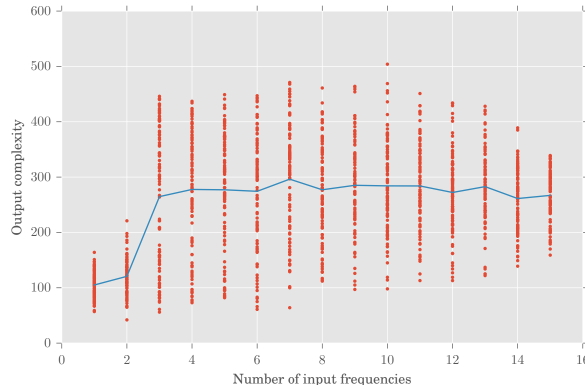

(b) Material B15S03 (1.25 wt% SWCNT)

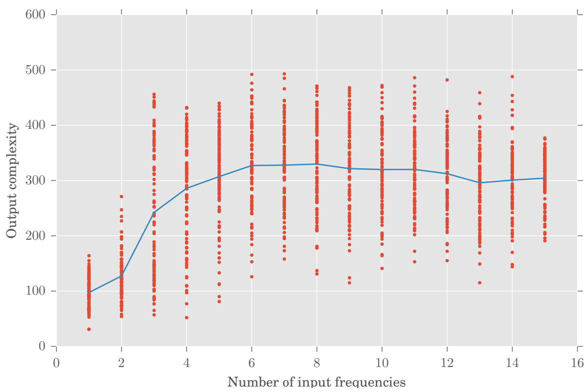

(c) Material B15S04 (1.50 wt% SWCNT)

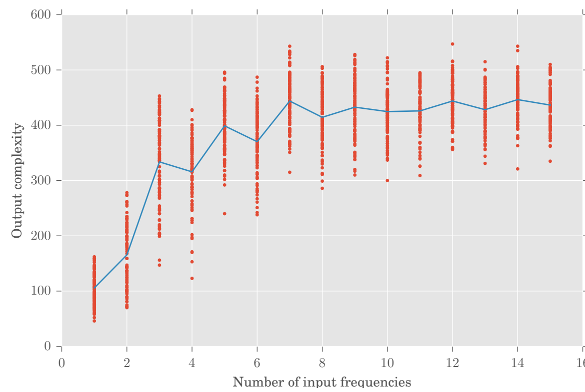

(d) Material B15S08 (5.00 wt% SWCNT)

Figure 8. Output complexity as the number of input frequencies are increased from 1 to 15 for four different material samples. The red scatter plot shows individual measurements while the blue line indicates the mean values for each of the 100 data points.

A. *Experimental Setup*

For all the experiments, a set of input signals are sent through the material and a single output signal is recorded. The input signals are digital square waves in the range $400Hz$ to $25kHz$. The amplitude of the square waves is $0 - 3.3V$, which means that the material is exposed to a sharp rise and fall of the signal in this range. The duty cycle is held constant at 50%.

The output signal is recorded as analog voltage over time and sampled at a frequency of $500kHz$ for 10ms resulting in an output buffer of 5000 samples.

In order to compare the analog output signal to the digital input signal, we digitize the output signal by using the mean voltage as digital threshold. In other words, samples above the mean correspond to logical 1 and samples below the mean correspond to logical 0. To reduce sensitivity to noise, we apply hysteresis so that transitions between logic levels happen only if the analog voltage crosses the mean by a noise margin.

Complexity is estimated by compressing the sample buffer with zlib (zlib is based on LZ77 [36]) and calculating the length of the compressed string. Input complexity C_i is calculated based on a set of ideal square waves sampled at the same frequency as the output signal ($500kHz$).

All the experiments are repeated for the different material samples listed in Table I.

1) Complexity as number of input signals are increased: In the first experiment, the number of input pins are increased from 1 to 15. Input pins are selected at random and for each input pin a random frequency is chosen in the range of $400Hz - 25kHz$. The output signal is recorded from pin #0. The experiment is repeated 100 times for each number of input pins resulting in 1500 output signals.

2) Complexity as function of one input frequency: The second set of experiments provides a more detailed view of a subset of the first experiment by traversing the input frequency spectrum. Frequencies are increased from $400Hz - 25kHz$ in steps of $1000Hz$ resulting in 25 different input frequencies. The number of input pins are again increased from 1 to 15 but the same frequency is now applied to all input pins. In addition, both input pins and output pins are selected at random. For each number of input pins and for each frequency, the experiment is repeated 100 times resulting in 37500 output signals.

3) Complexity as function of two input frequencies: In the third experiment, we again traverse the same input frequency spectrum ($400Hz - 25kHz$), but this time for two input pins. In other words, the frequency spectrum is traversed in

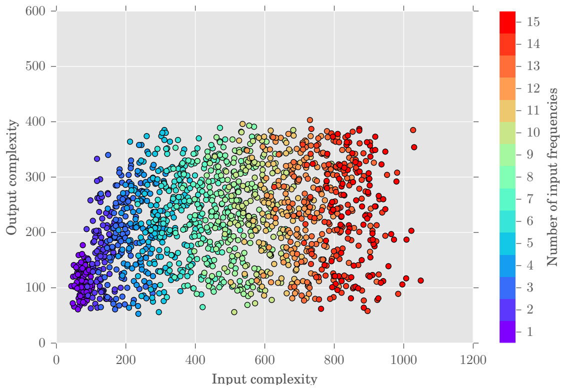

(a) Material B09S12 (0.53 wt% SWCNT)

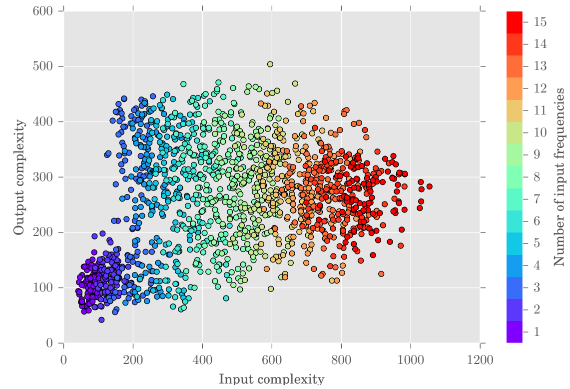

(b) Material B15S03 (1.25 wt% SWCNT)

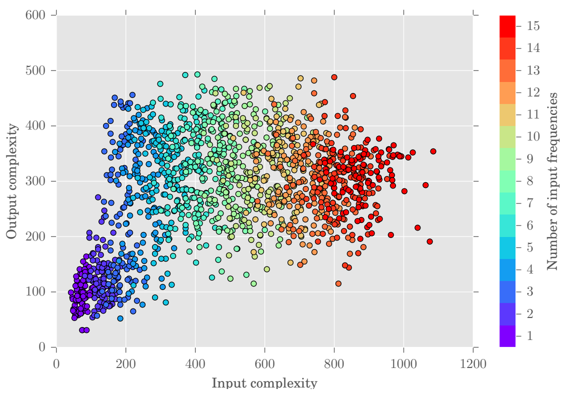

(c) Material B15S04 (1.50 wt% SWCNT)

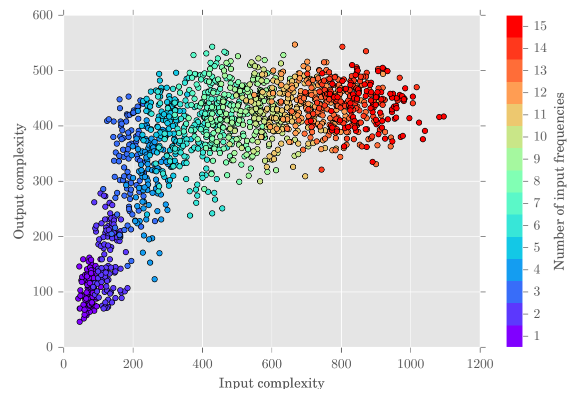

(d) Material B15S08 (5.00 wt% SWCNT)

Figure 9. Input vs output complexity as number of input frequencies are increased from 1 to 15 for four different material samples. The dots are colored according to the number of input frequencies used.

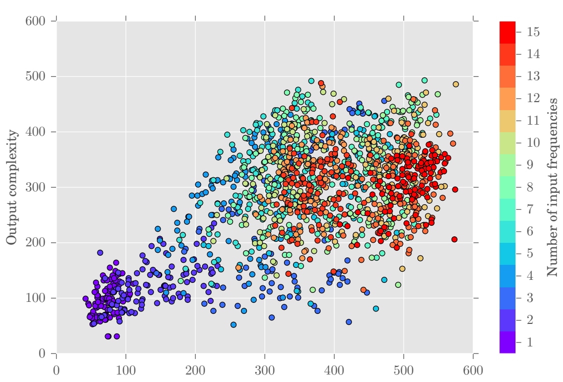

(a) Material B15S04 (1.50 wt% SWCNT)

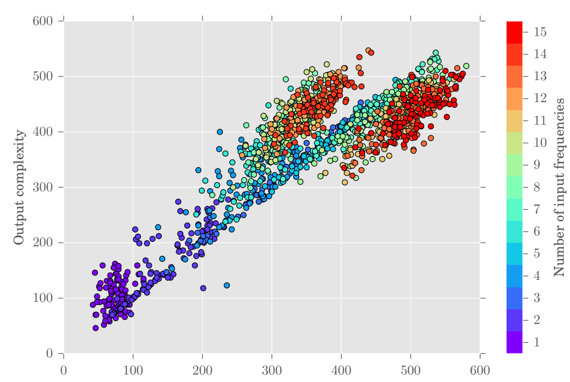

(b) Material B15S08 (5.00 wt% SWCNT)

Figure 10. Input vs output complexity when the input signals are summed together before input complexity is estimated. Results from two material samples with different SWCNT concentrations are shown. The dots are colored according to the number of input frequencies used.

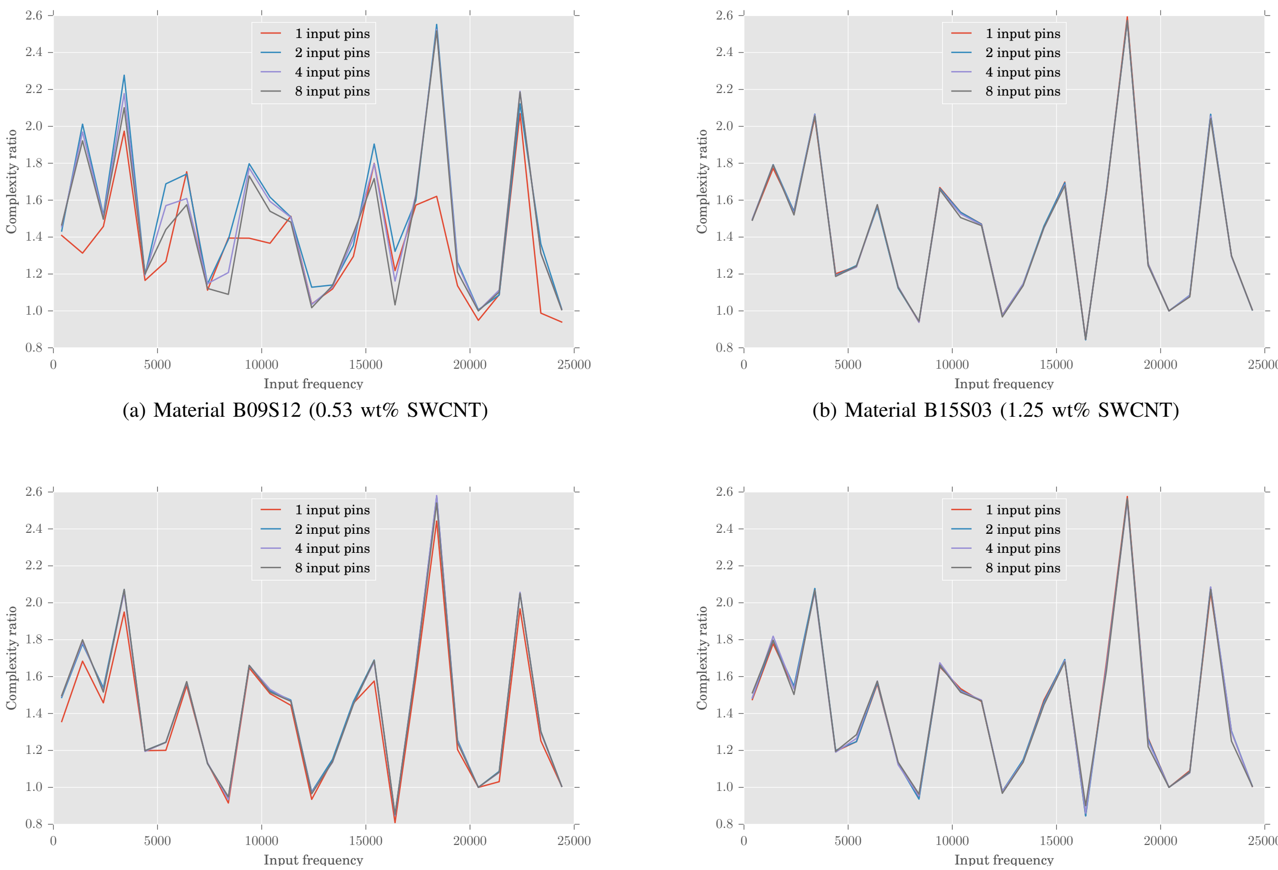

(a) Material B09S12 (0.53 wt% SWCNT)

(b) Material B15S03 (1.25 wt% SWCNT)

(c) Material B15S04 (1.50 wt% SWCNT)

(d) Material B15S08 (5.00 wt% SWCNT)

Figure 11. Mean complexity ratio as function of input frequency for 1, 2, 4 and 8 input pins. The same frequency is applied to all input pins. Results from four different material samples are shown.

two dimensions resulting in 25^2 pairs of input frequencies. Both input pins and output pins are selected at random. The experiment is repeated 10 times for each set of input/output pins.

B. Results and discussion

1) Complexity as number of input signals are increased: Figure 8 shows output complexity C_o measured over the range of 1-15 input frequencies. The blue line shows the mean output complexity value for each of the 100 data points. As shown in the plots, the output complexity increases with the number of input signals. There appears to be a fairly sharp rise in complexity as the number of square wave inputs are increased from 1 to 4. After this point the output complexity appears to saturate.

The scatter plot shows a fairly high variation in output complexity when the number of input signals exceeds one. This indicates that the materials exhibit a rich variety in output depending on the frequency and/or the choice of input pins.

A more detailed view is obtained when output complexity is plotted against input complexity (Figure 9). In these plots, it becomes clear that the input complexity C_i increases almost linearly with the number of input signals. Output complexity, however, saturates quickly above 3-4 input signals. In other words, above this level the added complexity from the input signal is not observed at the output.

Again the richness of output complexity can be observed. The output signal is generally less complex than the input signal, which indicates that the material acts as a filter or stable attractor. However, there are situations where the complexity of the output signal exceeds that of the input signal. The input complexity is estimated from *ideal* square waves, which are not directly comparable to the signals generated by the hardware platform. However, the estimate does give an indication that the materials exhibit rich dynamics.

From Figures 8 and 9 it appears as if higher concentrations of SWCNTs result in higher output complexity. Such a trend is counter-intuitive, since as concentration increases the electrical resistance of the material is reduced. As resistance goes towards zero the material should act more like a wire, which means that the input signals should pass through unaltered. If multiple input signals are sent through a wire, the output signal would simply be the sum of the input signals. Therefore, it would be interesting to investigate how closely the output signal resembles the sum of the input signals.

Figure 10 plots input vs output complexity when the input signals are summed together before C_i is estimated. For the material with high SWCNT concentration (B15S08, Figure

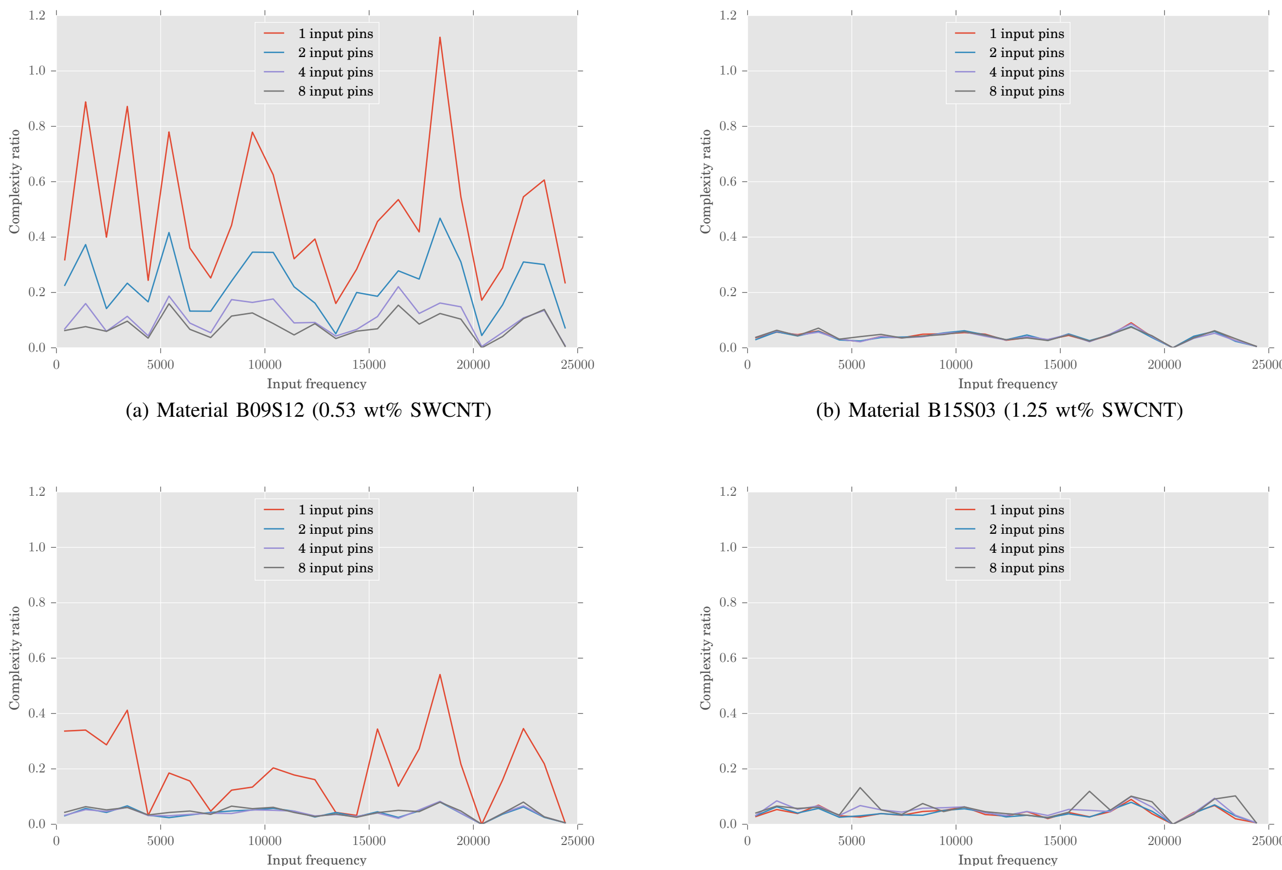

(a) Material B09S12 (0.53 wt% SWCNT)

(b) Material B15S03 (1.25 wt% SWCNT)

(c) Material B15S04 (1.50 wt% SWCNT)

(d) Material B15S08 (5.00 wt% SWCNT)

Figure 12. Standard deviation of complexity ratio as function of input frequency for 1, 2, 4 and 8 input pins. The same frequency is applied to all input pins. Results from four different material samples are shown.

10b) there is now a clear linear relationship between input complexity and output complexity. In other words, this material appears to behave much like a wire that simply sums the input signals together in some way. Lower SWCNT concentrations, however, display more diverse behavior as can be seen in Figure 10a, where there is no clear linear relationship between C_i and C_o.

2) Complexity as function of one input frequency: Figure 11 shows the mean *complexity ratio* C_r over the range of input frequencies applied to the four material samples. From the plots it is evident that C_r is highly dependent on the input frequency with spikes at certain frequencies. Complexity appears to be fairly consistent across the four material samples, i.e., the materials are sensitive to the same frequencies.

Applying the input frequency to more pins does not seem to affect the mean complexity by much. However, there is a clear reduction in complexity variation, as can be seen from Figure 12, where standard deviation of the complexity ratio is shown. One possible explanation is that the input signal is effectively amplified as it is applied to more input pins.

Another trend that can be seen from the plots in Figure 12 is an inverse relationship between complexity variation and the SWCNT concentration, i.e., more uniform output complexity with increased SWCNT concentration. This may be due to the fact that higher SWCNT concentration leads to a lower electrical resistance in the material and thus more pathways for the input signal to reach the output pin. However, one exception can be observed for the B15S04 sample where a higher variation is found when the frequency is applied to only one input pin. This likely indicates that one electrode is only partially connected to the material in this particular sample.

3) Complexity as function of two input frequencies: By sweeping the two input frequencies applied to the material we get a more detailed view of some of the results from the first experiment. Figure 13 depicts complexity ratio as a heat map where the two input frequencies are swept in the X and Y axes and color represents complexity. The colors range from dark purple (low complexity) to bright yellow (high complexity). As with one input signal, the heat maps show clearly that the complexity landscape is dependent on the selection of input frequencies.

Figures 13a and 13b depict complexity for the same material sample B09S12, but with different selection of input and output pins. As can be seen, the two heat maps display clear differences in complexity ratio, where the latter pin configuration (13b) generally exhibits more complex output. However, this is not always the case, as can be seen in Figures 13c and 13d, where different input locations result in quite

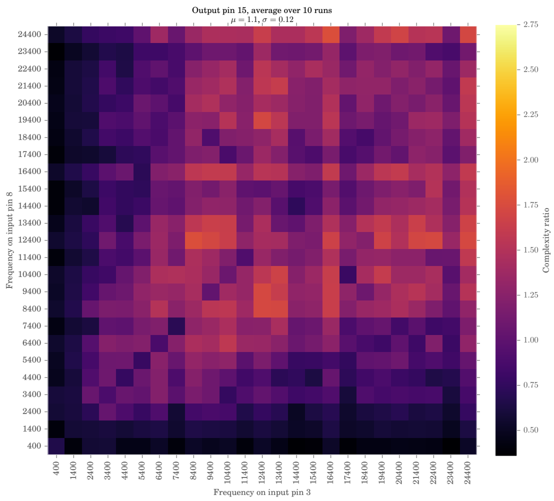

(a) Material B09S12 (0.53 wt% SWCNT), input pins 3 and 8, output pin 15

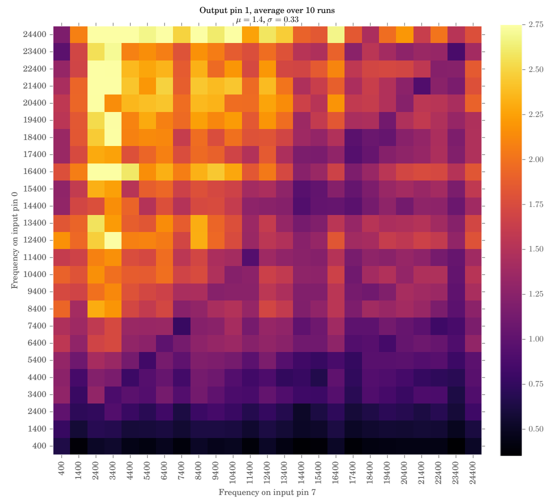

(b) Material B09S12 (0.53 wt% SWCNT), input pins 7 and 0, output pin 1

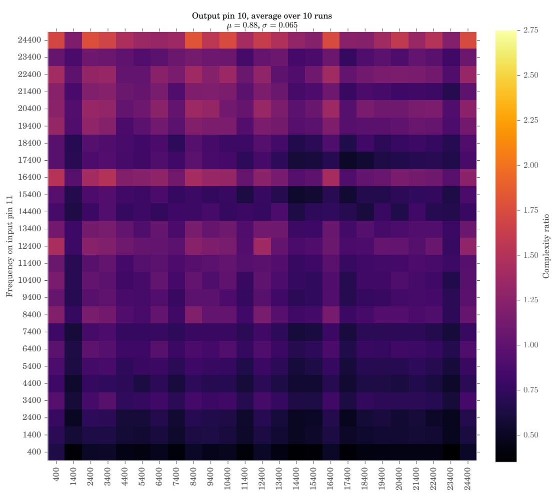

(c) Material B15S08 (5.00 wt% SWCNT), input pins 12 and 11, output pin 10

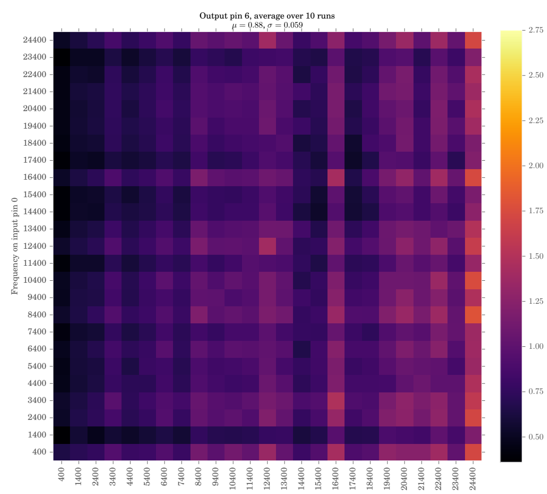

(d) Material B15S08 (5.00 wt% SWCNT), input pins 10 and 0, output pin 6

Figure 13. Complexity ratio as function of two input frequencies (X and Y axes). The heat maps shows complexity ratio C_r averaged over 10 runs. Colors range from dark purple (low complexity) to bright yellow (high complexity). Four heat maps are shown for two material samples: B09S12 (13a-13b) and B15S08 (13c-13d). Each heat map shows complexity when input is applied to different input/output pins.

similar complexity landscapes.

VI. Conclusion

The general ideas, experiments, and results presented relates to dynamics performed by SWCNT and PBMA nanocomposites, which may be exploited by EIM. The materials and experimental system (as presented in Section II) has shown promising computational behavior on a variety of problems. In this work, the behaviors are related to measurable dynamic behavior. That is, the experiments are designed to capture dynamic properties of the materials as to gain an understanding of what inherent dynamics are observable in an EIM setting. The approach taken is to view the material, i.e., physical system, as a hierarchical information processing device (Figure 2). At the bottom level the physical dynamics, i.e., quantum effects due to mechanisms of electron transmission through carbon nanotubes, are not observable within a reasonable resource usage. As such, the lowest level is treated only at a conceptual level. Dynamics at the bottom level are only observed as resulting voltages in the analogue domain. The information available at this level is exploited to gain insight into the electrical properties of the material when exposed to dynamic input stimuli. At the top level the material is interpreted as a discrete dynamical system. However, the observable dynamics at this discrete level is a result of all the underlying physics.

As stated by Miller et al. [3]: "...exploit the intrinsic properties of materials, or "computational mediums", to do computation, where neither the structure nor computational properties of the material needs to be known in advance". The statement may indicate that any material can be looked at as a black-box. However, insight into what properties are available for evolution provides knowledge on how to construct a successful EIM system. Our findings show that the materials exhibit rich dynamical properties observable at the analogue level. Figure 7 shows the behavior at an (close to) analogue time and voltage scale. The properties of these behaviors are available for exploitation by evolution, even if not explicitly controllable from the top discrete digital domain.

At the top level, the abstract measurements of complexity shows how such a measurement can indicate what computational problems the EIM system may handle. Especially, the experimental results from Figure 13 show that the materials tested include behavior found in classifier systems, such as Thompson's frequency discriminator [5] (generally a trend of reduced complexity as illustrated in Figure 13d). From the same experiment, Figure 13b shows an increase in complexity generated by the dynamics of the material. A clear indication of a system which has more internal (observable) states than of the input data.

Our results also reveal several specific properties of the SWCNT materials used. In particular, as the number of input signals grows, a saturation of output complexity is reached. From an EIM perspective this is interesting, since it implies that information is filtered when many input signals are applied. The results also show a wide variety in output complexity depending on input frequency and selection of input/output pins. An indication that the materials are capable of many different modes of operation.

Acknowledgment

The research leading to these results has received funding from the European Community's Seventh Framework Programme (FP/2007-2013) under grant agreement number 317662.

References

[1] S. Nichele, D. Laketić, O. R. Lykkebø, and G. Tufte, "Is there chaos in blobs of carbon nanotubes used to perform computation?" in FUTURE COMPUTING 2015, The Seventh International Conference on Future Computational Technologies and Applications. ThinkMind, 2015, pp. 12–17.

[2] H. Broersma, F. Gomez, J. Miller, M. Petty, and G. Tufte, "Nascence project: nanoscale engineering for novel computation using evolution," International journal of unconventional computing, vol. 8, no. 4, 2012, pp. 313–317.

[3] J. Miller, S. Harding, and G. Tufte, "Evolution-in-materio: evolving computation in materials," Evolutionary Intelligence, vol. 7, no. 1, 2014, pp. 49–67.

[4] J. Miller and K. Downing, "Evolution in materio: Looking beyond the silicon box," in The 2002 NASA/DoD Conference on Evolvable Hardware, A. Stoica, J. Lohn, R. Katz, D. Keymeulen, and R. S. Zebulum, Eds., Jet Propulsion Laboratory, California Institute of Technology. Alexandria, Virginia: IEEE Computer Society, 15-18 July 2002, pp. 167–176.

[5] A. Thompson, Hardware evolution - automatic design of electronic circuits in reconfigurable hardware by artificial evolution. CPHC/BCS distinguished dissertations, 1998.

[6] S. Harding and J. Miller, "Evolution in materio : A real-time robot controller in liquid crystal," in Proceedings of the 2005 NASA/DoD Conference on Evolvable Hardware, J. Lohn, D. Gwaltney, G. Hornby, R. Zebulum, D. Keymeulen, and A. Stoica, Eds. Washington, DC, USA: IEEE Press, 29 June-1 July 2005, pp. 229–238.

[7] P. Cariani, "To evolve an ear: epistemological implications of Gordon Pask's electrochemical devices," Systems Research, vol. 10, no. 3, 1993, pp. 19–33.

[8] K. Clegg, J. Miller, K. Massey, and M. Petty, "Travelling salesman problem solved "in materio" by evolved carbon nanotube device," in Parallel Problem Solving from Nature - PPSN XIII, ser. Lecture Notes in Computer Science, T. Bartz-Beielstein, J. Branke, B. Filipic, and J. Smith, Eds. Springer International Publishing, 2014, vol. 8672, pp. 692–701.

[9] A. Kotsialos, K. Massey, F. Qaiser, D. Zeze, C. Pearson, and M. Petty, "Logic gate and circuit training on randomly dispersed carbon nanotubes." International journal of unconventional computing., vol. 10, no. 5-6, September 2014, pp. 473–497.

[10] M. Mohid, J. Miller, S. Harding, G. Tufte, O. R. Lykkebø, K. Massey, and M. Petty, "Evolution-in-materio: Solving bin packing problems using materials," in The 2014 IEEE Conference on Evolvable Systems - ICES, IN PRESS. IEEE Computer Society, 2014.

[11] M. Mohid, J. Miller, S. Harding, G. Tufte, O. Lykkebø, M. Massey, and M. Petty, "Evolution-in-materio: Solving machine learning classification problems using materials," in Parallel Problem Solving from Nature PPSN XIII, ser. Lecture Notes in Computer Science, T. Bartz-Beielstein, J. Branke, B. Filipic, and J. Smith, Eds. Springer International Publishing, 2014, vol. 8672, pp. 721–730.

[12] M. Mohid, J. Miller, S. Harding, G. Tufte, O. R. Lykkebø, K. Massey, and M. Petty, "Evolution-in-materio: A frequency classifier using materials," in The 2014 IEEE Conference on Evolvable Systems - ICES, IN PRESS. IEEE Computer Society, 2014, pp. 46–53.

[13] M. Mohid, J. Miller, S. Harding, G. Tufte, O. Lykkebo, M. Massey, and M. Petty, "Evolution-in-materio: Solving function optimization problems using materials," in Computational Intelligence (UKCI), 2014 14th UK Workshop on, D. Neagu, M. Kiran, and P. Trundle, Eds. IEEE, September 2014, pp. 1–8.

[14] A. N. Kolmogorov, "Three approaches to the quantitative definition of information," Problems of information transmission, vol. 1, no. 1, 1965, pp. 1–7.

[15] G. Pask, "Physical analogues to growth of a concept," Mechanisation of Thought Processes, 1959, pp. 877–922.

[16] R. Stewart, “Electrochemically active field-trainable pattern recognition systems,” Systems Science and Cybernetics, IEEE Transactions on, vol. 5, no. 3, 1969, pp. 230–237.

[17] J. W. Mills, “Polymer processors,” Technical Report TR580, Department of Computer Science, University of Indiana, Tech. Rep., 1995.

[18] S. L. Harding and J. F. Miller, “Evolution in materio: Computing with liquid crystal,” Journal of Unconventional Computing, vol. 3, no. 4, 2007, pp. 243–257.

[19] S. Harding and J. F. Miller, “Evolution in materio: A tone discriminator in liquid crystal,” in Evolutionary Computation, 2004. CEC2004. Congress on, vol. 2. IEEE, 2004, pp. 1800–1807.

[20] ——, “Evolution in materio: Evolving logic gates in liquid crystal,” in In Proceedings of the workshop on unconventional computing at ECAL 2005 VIIIth European. Beckington, UK, 2005, pp. 133–149.

[21] M. Mohid and J. Miller, “Evolving robot controllers using carbon nanotubes,” in The 2015 European Conference on Artificial Life. The MIT Press, 2015.

[22] T. Kowaliw, “Measures of complexity for artificial embryogeny,” in Proceedings of the 10th annual conference on Genetic and evolutionary computation. ACM, 2008, pp. 843–850.

[23] M. Li and P. Vitányi, An introduction to Kolmogorov complexity and its applications. Springer Science & Business Media, 2013.

[24] S. Nichele and G. Tufte, “Measuring phenotypic structural complexity of artificial cellular organisms,” in Innovations in Bio-inspired Computing and Applications. Springer, 2014, pp. 23–35.

[25] M. Hartmann, P. K. Lehre, and P. C. Haddow, “Evolved digital circuits and genome complexity,” in Evolvable Hardware, 2005. Proceedings. 2005 NASA/DoD Conference on. IEEE, 2005, pp. 79–86.

[26] P. K. Lehre and P. C. Haddow, “Developmental mappings and phenotypic complexity.” in IEEE Congress on Evolutionary Computation (1). Citeseer, 2003, pp. 62–68.

[27] H. Zenil and E. Villarreal-Zapata, “Asymptotic behavior and ratios of complexity in cellular automata,” International Journal of Bifurcation and Chaos, vol. 23, no. 09, 2013, p. 1350159.

[28] B. J. MacLennan, “A review of analog computing. technical report ut-cs-07-601,” University of Tennessee, Knoxville, Tech. Rep., 2007.

[29] H. J. Bremermann, Self-Organizing Systems-1962. Spartan Books, 1962, ch. Optimization through Evolution and Recombination, pp. 93–106.

[30] O. R. Lykkebø, S. Harding, G. Tufte, and J. Miller, “Mecobo: A hardware and software platform for in materio evolution,” in Unconventional Computation and Natural Computation - 13th International Conference, UCNC 2014, London, ON, Canada, July 14-18, 2014, Proceedings, 2014, pp. 267–279.

[31] A. S. Foundation, “Apache thrift,” accessed: 2016-06-07. [Online]. Available: https://thrift.apache.org/

[32] W. R. Ashby, Design for a Brain, the origin of adaptive behaviour. Chapman & Hall Ltd., 1960.

[33] L. von Bertalanffy, General System Theory. George Braziller, Inc., Revised edition, Fourth printing, 1973.

[34] D. Laketić, G. Tufte, S. Nichele, and O. R. Lykkebø, “An explanation of computation - collective electrodynamics in blobs of carbon nanotubes,” in Proceedings of the 9th EAI International Conference on Bio-Inspired Information and Communications Technologies (formerly BIONETICS). EAI, ACM Digital Library, 2015.

[35] O. R. Lykkebø, S. Nichele, and G. Tufte, “An investigation of square waves for evolution in carbon nanotubes material,” Proceedings of the European Conference on Artificial Life, 2015, pp. 503–510.

[36] J. Ziv and A. Lempel, “A universal algorithm for sequential data compression,” IEEE Transactions on Information Theory, vol. 23, no. 3, May 1977, pp. 337–343.